Turkish Journal of Physics
http://journals.tubitak.gov.tr/physics/
Research Article

Turk J Phys
(2018) 42: 443 – 454
© TÜBİTAK
doi:10.3906/fiz-1803-28

Size- and composition-dependent structure of ternary Cd-Te-Se nanoparticles

Mustafa KURBAN*
Department of Electronics and Automation, Ahi Evran University, Kırşehir, Turkey

Received: 26.03.2018 • **Accepted/Published Online:** 22.06.2018 • **Final Version:** 15.08.2018

Abstract: In this study, the geometrical, thermal, and energetic properties of zinc-blende $CdTe_{1-x}Se_x$ (x = 0.25, 0.50, and 0.75) nanoparticles were investigated using the bond order potential based on the modern classical molecular dynamics (MD) method. All MD simulations were performed using LAMMPS. Some physical properties were investigated, such as compositional variations of Cd, Te, and Se atoms; order parameter; radial distribution function; coordination number; potential energy; and heat capacity (C_v). The simulation results were compared with the available experimental results. The obtained results revealed that an increase in the composition of Se atoms can provide contributions to stability, which is desirable to increase the efficiency of solar cells.

Key words: Nanoparticles, radial distribution function, coordination number, heat capacity, molecular dynamics

1. Introduction

Nanoparticles (NPs) have been the subject of many applications including energy, electronics, biomedicine, and optical fields due to their excellent size- and shape-dependent properties differing based on their bulk materials. NPs can be classified into different groups based on their type such as metal, semiconductor, insulator, or organic. Among these types, semiconductor NPs have been widely investigated because the materials have been found useful in important applications [1–3]. In particular, Cd-based compounds such as CdTe, CdSe, CdZnTe, and CdTeSe are used in detectors, transistors, solar cells, and optoelectronic devices [4–8]. Recently, ternary alloy $CdTe_{1-x}Se_x$ compounds have received a great deal of attention when compared with binary CdTe and CdSe and ternary CdZnTe compounds for the following reason: $CdTe_{1-x}Se_x$ ternary alloys meet the requirements of solar cells, photoconductors, and thin-film transistors because their absorption spectra can be adjusted from the blue to the red regions [9]. However, CdTe and CdSe binary alloys do not work well for emission for the blue region [10]. The electron effective mass of binary CdTe alloy is also more than that of ternary CdTeSe, and thus the mobility of CdTe is expected to be lower than that of CdTeSe [11]. Furthermore, solidification segregation is encountered as a problem during the growth of ternary $Cd_{1-x}Zn_xTe$ alloys at high temperature due to radial variations in segregation [12]. However, CdTeSe has the near-unity (0.98) segregation coefficient of Se, and thus it is distributed uniformly in the CdTe matrix [13]. This provides a considerable increase in the yield of detector-grade material [14]. In a recent study, researchers showed that $CdTe_xSe_{1-x}$ alloy layer photoactivity provides a crucial contribution for improving CdTe-based solar cells [15]. Moreover, the short circuit current densities of CdTe cells in both the short and long wavelength regions can be enhanced using CdSe window layers (a cell efficiency of 14.7%) due to the composition of Se atoms [16]. CdSeTe solid solution hardening with Se is also more effective than that of CdZnTe with Zn.

*Correspondence: mkurbanphys@gmail.com

All the examples mentioned above indicate the role of the CdTeSe compound and invite further investigation about this material. Recently, we studied the physical properties of CdZnTe nanowires, nanoparticles, and clusters by Lennard-Jones with two-body interactions [17] and the Axilrod–Teller triple-dipole function with three-body interactions [18], bond order potential (BOP), and density functional theory (DFT) calculations [19–24]. To our knowledge, there is no study on the size and composition dependence properties of Cd-Te-Se NPs in the literature. Thus, the major aim of the present study was to probe the compositional variations of Cd, Te, and Se atoms together with the order parameter (R), radial distribution function (RDF), coordination number, potential energy, and heat capacity (C_v) of zinc-blende $CdTe_{1-x}Se_x$ NPs.

2. The method of calculations

A modern version of molecular dynamics (MD) simulations with LAMMPS [25,26] was performed using Cd-Te-Se ternary analytical BOP [27]. The BOP formalism was constructed from CdTe BOP [28,29]. A total of 82 parameters were defined for the BOP. The details on the physics and parameterization of the BOP were given in previous works [30–33].

In the simulations, a Nosé–Hoover thermostat [34,35] (in NVT ensemble) is used to control the thermal equilibrium of the system. The energetic relaxation is performed at fixed geometry (stable structure). The simulations are carried out starting at 1 K and the temperature of the system is increased by 25 K up to 800 K. The system is relaxed at every temperature rise for about 0.1 ns. The system is gradually annealed (25 K) without waiting for thermal equilibrium. The initial velocities are determined from the Boltzmann distribution. The effective cutoff is taken as 14.70 Å since the BOP of many-body calculations involve neighbors of neighbors of neighbors. As an example, initial views of the $CdTe_{1-x}Se_x$ (x = 0.50) NPs' obtained zinc-blende structure are shown in Figure 1.

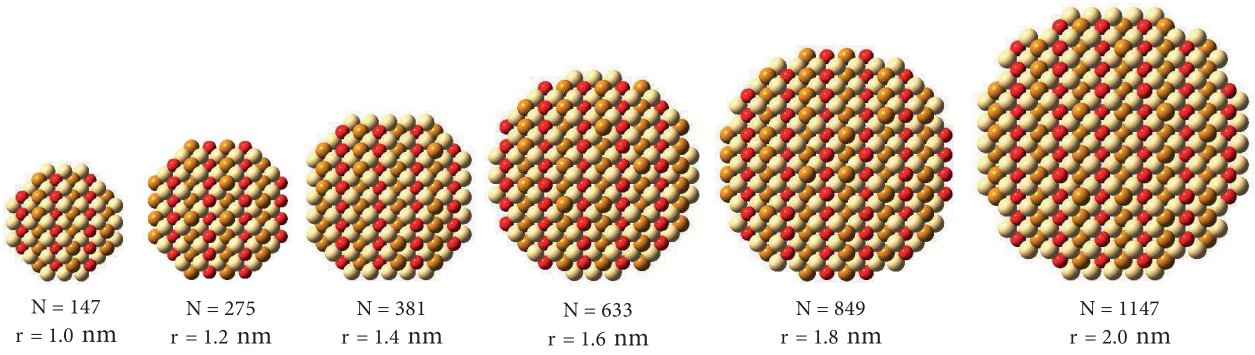

Figure 1. The generated views of the modeled $CdTe_{0.50}Se_{0.50}$ NPs (Cd is gray, Te is orange, and Se is red).

3. Results and discussion

To understand the segregation formation and size and composition dependence properties of the $CdTe_{1-x}Se_x$ (x = 0.25, 0.50, and 0.75) NPs, we analyzed the compositional variations of Cd, Te, and Se atoms as well as the order parameter, radial distribution function, potential energy, and heat capacity (C_v) and compared the results with the experimental ones in the literature.

Figures 2a and 2b respectively show the number of Te and Se atoms in the $CdTe_{1-x}Se_x$ (x = 0.25, 0.50, and 0.75) NPs as a function of the NP size. In Figure 2, the increase in the NP size is relatively slower up

to 1.4 nm, and then further increase in NP size from 1.4 to 2.0 nm is observed. This increment in the NP size is related to the shape of the NPs. This behavior can also be explained by the composition of Te and Se atoms in the NPs. The behavior of Te and Se atoms in Figures 2a and 2b is compatible with that of a recent experimental study at nanoscale [15]. In this recent experimental study, $CdTe_xSe_{1-x}$ layer photoactivity, which increases the efficiency of solar cells, was found to be extremely dependent on the composition of Te and Se atoms. Researchers also showed that Se atoms have a significant effect on the stability of $CdTe_{1-x}Se$ quantum dots [36].

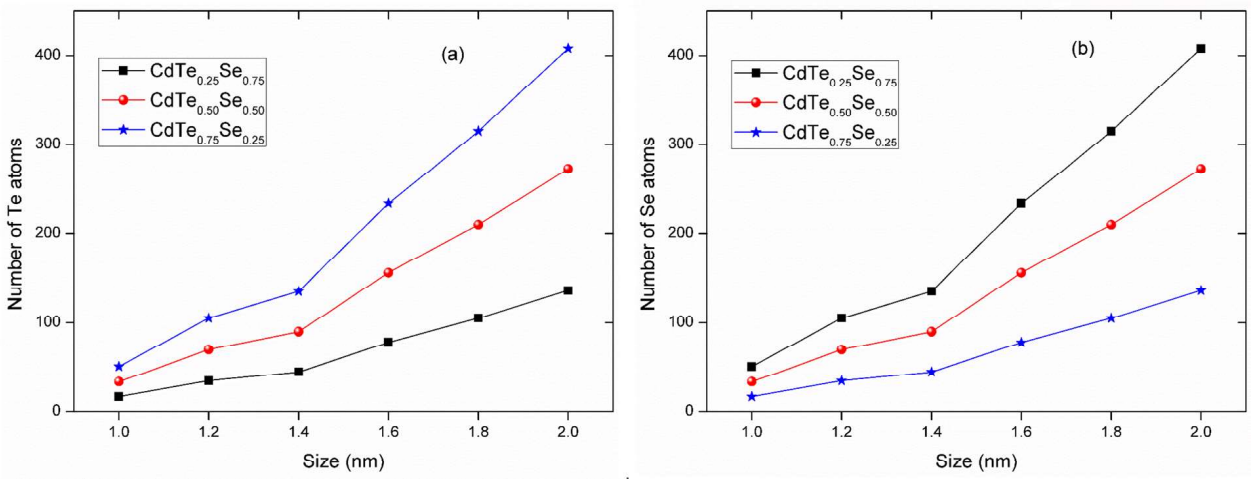

Figure 2. Number of the Te (a) and Se (b) atoms in the $CdTe_{1-x}Se_x$ (x = 0.25, 0.50, and 0.75) NPs as a function of NP size.

The formation of a stable structure for $Cd_{1-x}Zn_xTe$ is one of the major problems [12] to get high efficiency solar cell devices. Atom distribution in crystalline structures is uniform and homogeneous in general [37]. This behavior may not be conserved at nanoscale, especially under heat treatment [21]. Thus, the order parameter (R_A) is calculated to research the stable structure in NPs by analyzing the distribution of the different types of atoms [38]. R_A is identified by the average distance of type A atoms in accordance with the center of an NP,

$$R_A = \frac{1}{n_A}\sum_{i=1}^{n_A} r_i,$$

where n_A is the number of A type atoms in the ternary ABC NPs and r_i is the distance of the atoms to the coordinate center of the NP. If R_A is a small value, it means that A type atoms are at the center; if R_A is a large value, it means that A type atoms are at the surface region of the NP; and if R_A is a medium value, it means a well-mixed NP.

Figures 3a–3c show the behavior of R of Cd, Te, and Se atoms according to the NP size for $CdTe_{1-x}Se_x$ NPs (x = 0.25, 0.50, and 0.75). Cd atoms are on the surface as a general trend. The segregation of Cd atoms to the surface can be expressed as the lower cohesive energy of Cd atoms, and thus they move away from the inner regions of the NPs to the surface regions. Te and Se atoms are found to be at the center. The behavior of some incorporation of Te and Se inside the core has also been observed experimentally at nanoscale [39]. Taking into consideration the compositional dependence of R, $CdTe_{0.75}Se_{0.25}$ has a larger value than that of $CdTe_{0.25}Se_{0.75}$ and $CdTe_{0.50}Se_{0.50}$. Figures 4–6 show the behavior of R with respect to the temperature in

the 1.0–2.0 nm range for the Cd-Te-Se NPs. In general, it has the same behavior, except for the NP with 1.2 nm. It is interesting that Te atoms are on the surface because the distributions of the Te and Se atoms are segregated in the surface of the NP. It is less stable than the other NPs. In addition, depending on the NP size, the increment of R is becoming more stable than that of the other NPs under heat treatment.

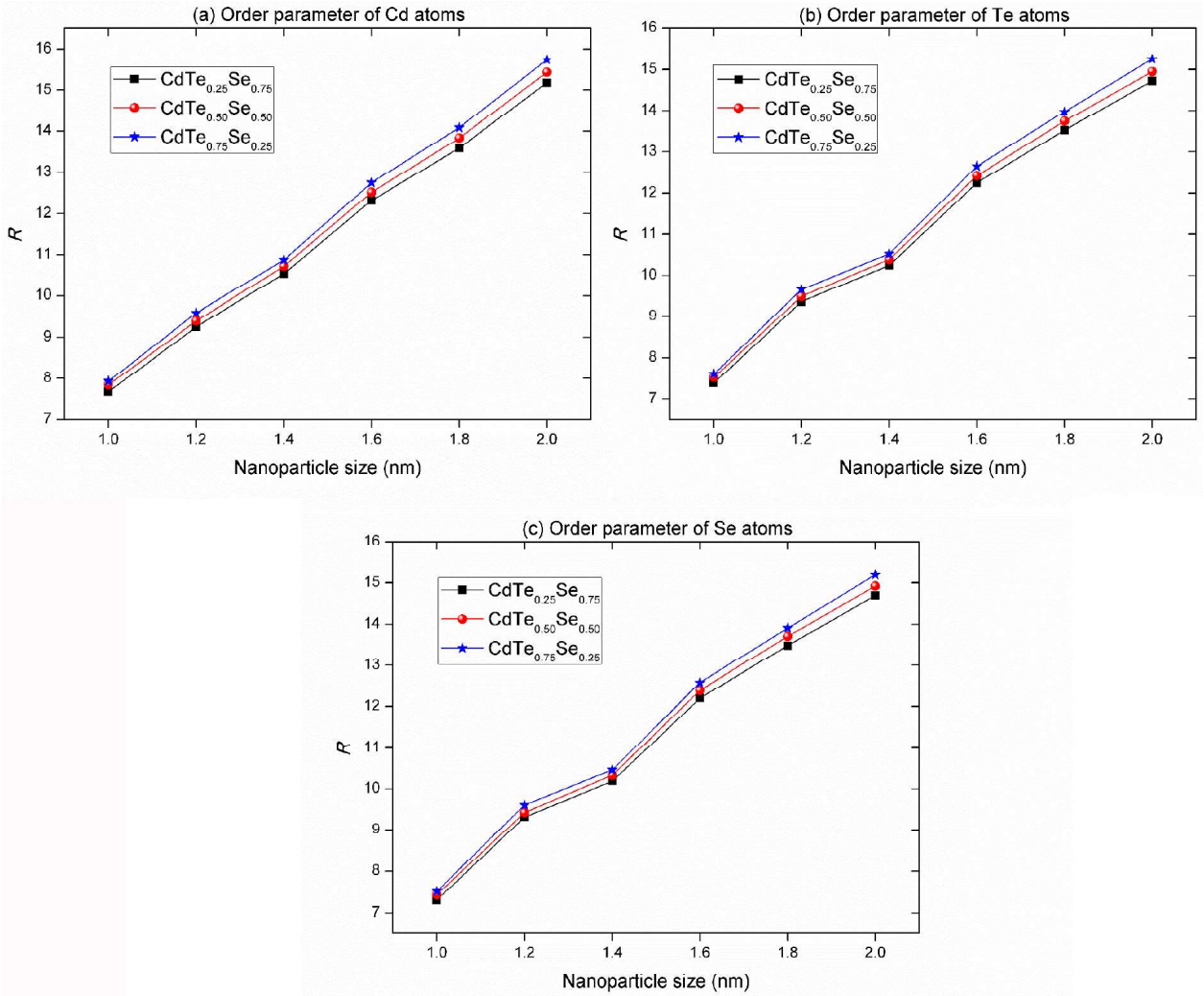

Figure 3. Behavior of the order parameter of Cd (a), Te (b), and Se (c) atoms according to size for $CdTe_{0.25}Se_{0.75}$, $CdTe_{0.50}Se_{0.50}$, and $CdTe_{0.75}Se_{0.25}$.

To study the influence of interactions of the atoms in the NPs, we calculated the probability distribution depending on the coordination number (Figure 7). The coordination number of all the interactions increases in line with the rise in temperature. Figures 8a–8d respectively show the radial distribution functions of the cadmium-cadmium (Cd-Cd), cadmium-tellurium (Cd-Te), cadmium-selenium (Cd-Se), tellurium-tellurium (Te-Te), tellurium-selenium (Te-Se), and tellurium-selenium (Se-Se) interactions of $CdTe_{0.50}Se_{0.50}$ NP with 2.0 nm at 100 K, 300 K, 500 K, and 800 K. The RDFs are calculated for each atomic pair of the optimized $CdTe_{0.50}Se_{0.50}$. One can see that Cd-Se has a narrower and higher distribution than the other pair interactions because of the weaker bond [27] and the low atomic weight of the Se atom. In addition, there is a slight difference

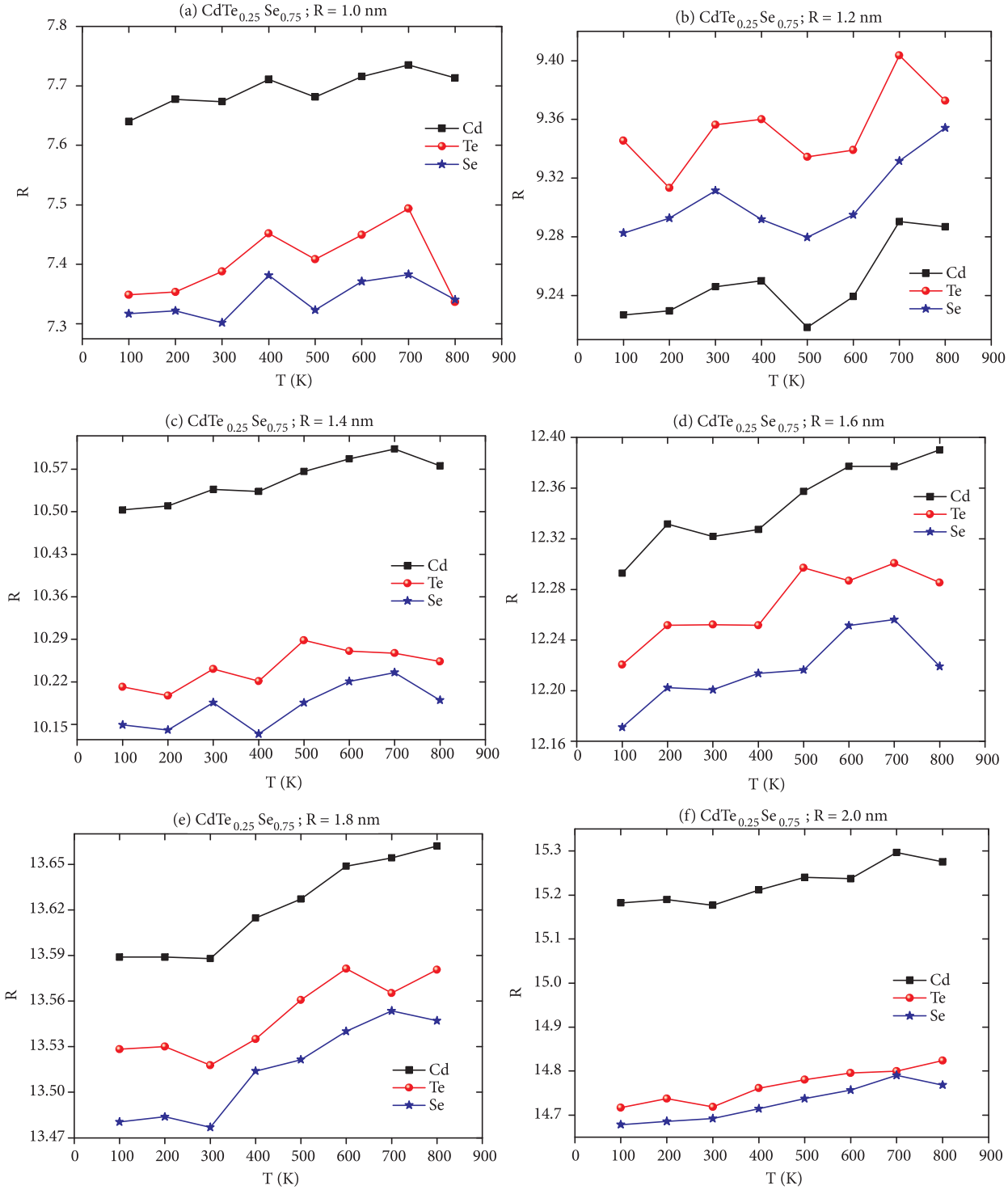

Figure 4. Behavior of the order parameter of Cd, Te, and Se atoms according to temperature for $CdTe_{0.25}Se_{0.75}$.

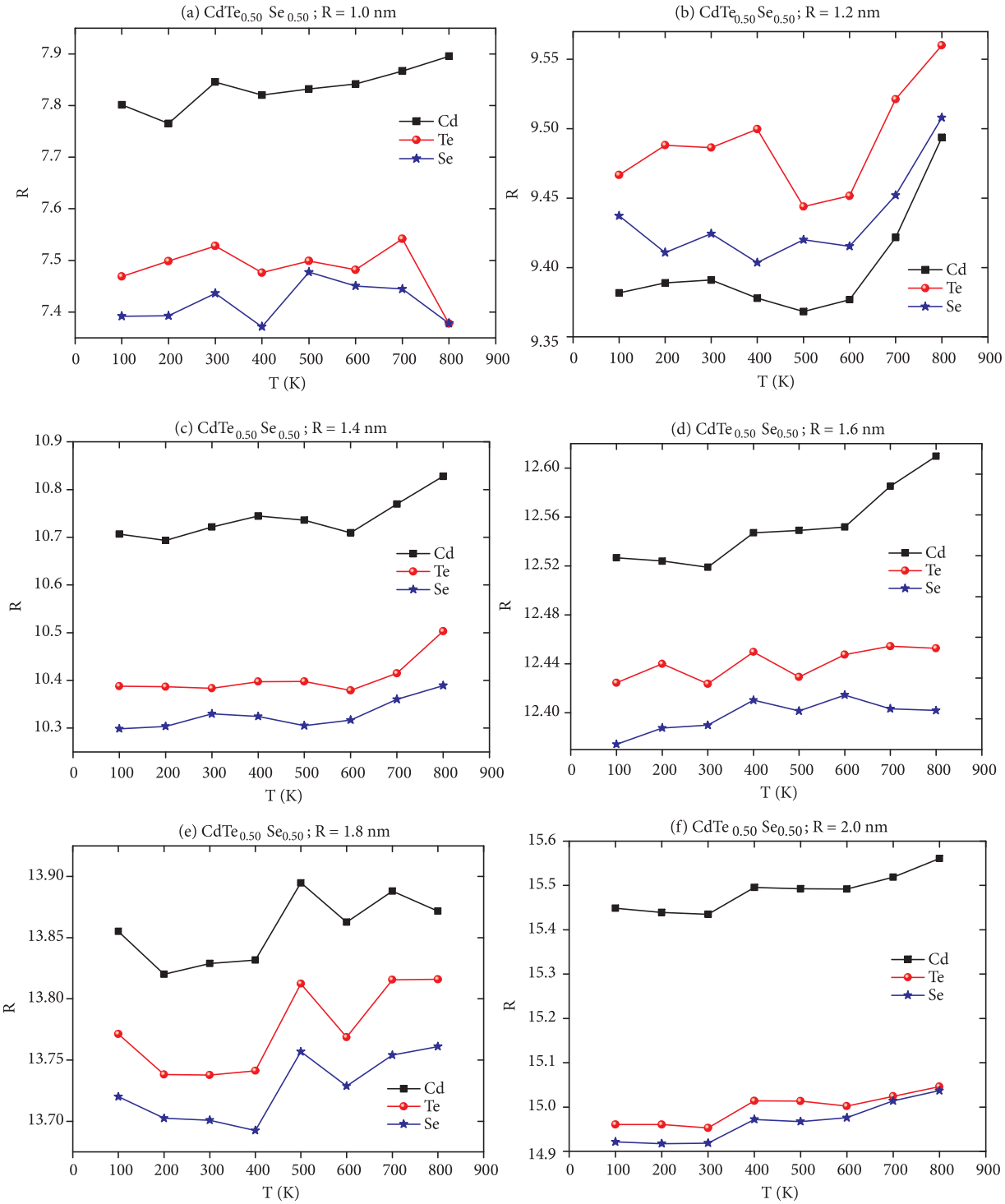

Figure 5. Behavior of the order parameter of Cd, Te, and Se atoms according to temperature for $CdTe_{0.50}Se_{0.50}$.

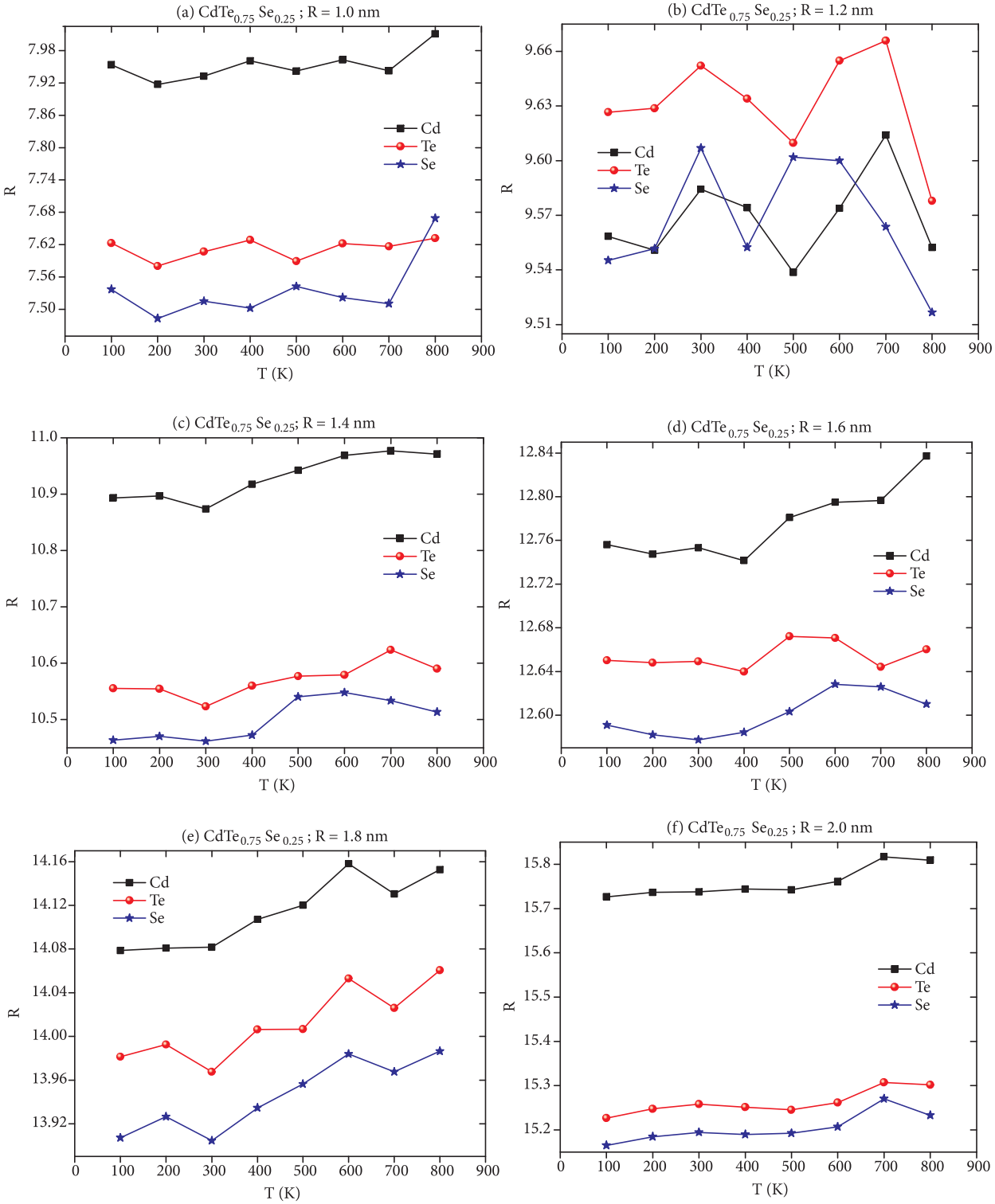

Figure 6. Behavior of the order parameter of Cd, Te, and Se atoms according to temperature for $CdTe_{0.75}Se_{0.25}$.

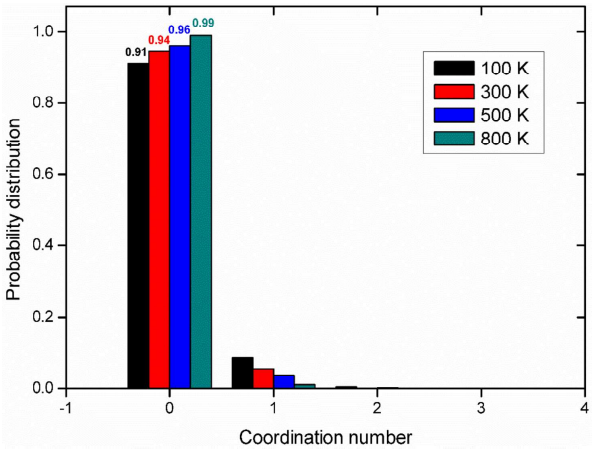

Figure 7. Probability distributions of all the coordination numbers in $CdTe_{0.50}Se_{0.50}$ NP for $R = 2.0$ nm at different temperatures.

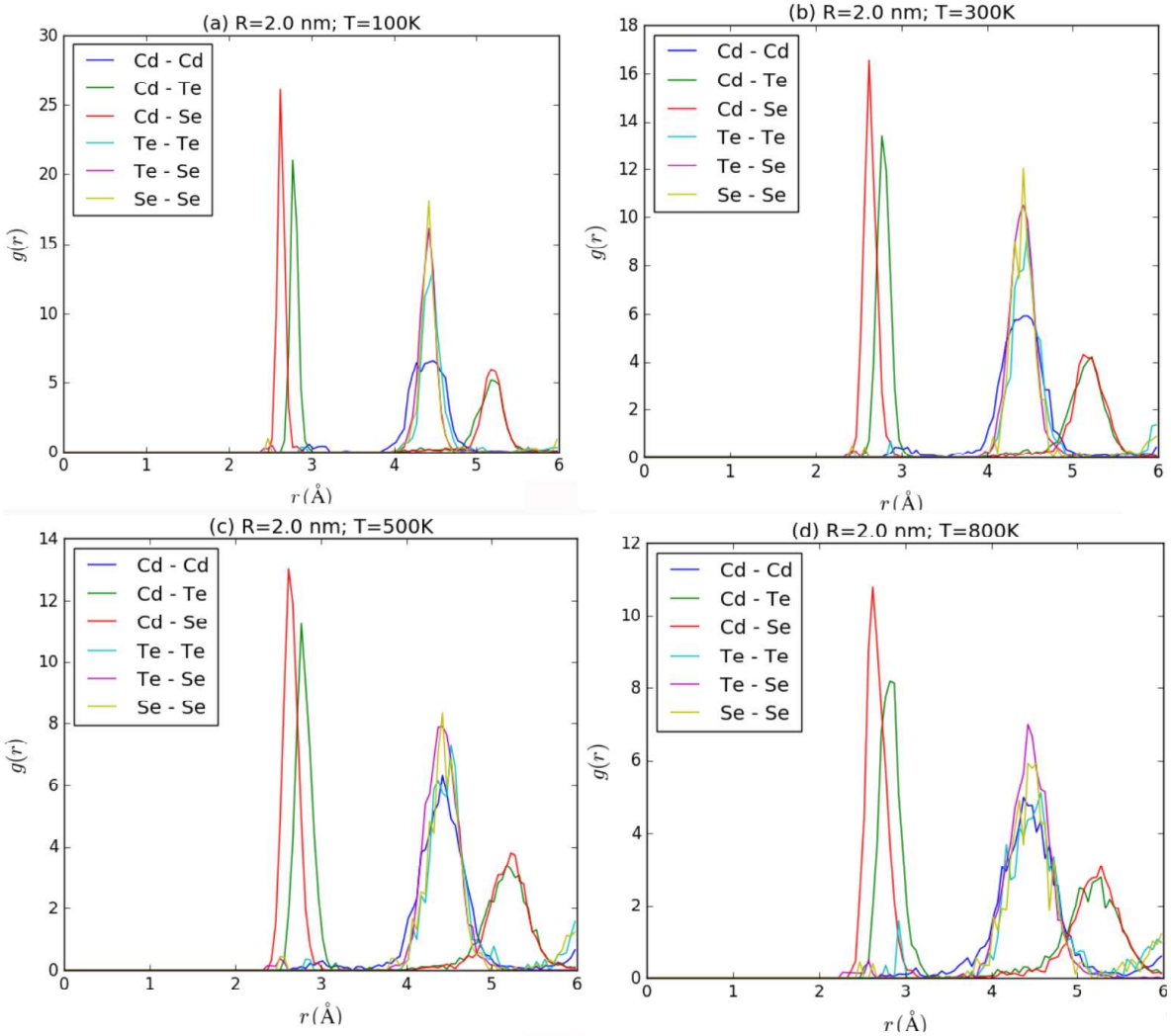

Figure 8. The RDFs of the Cd-Cd, Cd-Te, Cd-Se, Te-Te, Te-Se, and Se-Se interactions of $CdTe_{0.50}Se_{0.50}$ NP with 2.0 nm at (a) 100 K, (b) 300 K, (c) 500 K, and (d) 800 K.

between Te-Se and Se-Se atoms. For Cd atoms, Cd-Cd is shorter than Cd-Te and Cd-Se interactions; for Te, Te-Te is slightly shorter than Te-Se. For all the combinations, Cd-Se has stronger interactions than those of the others. The fluctuations of obvious peaks in RDFs also increase with the rising temperature.

Figure 9 represents the structures of the $CdTe_{0.50}Se_{0.50}$ spherical NP with 2.0 nm at 100 K, 300 K, 500 K, and 800 K. In Figure 9, Cd atoms move away from the inner regions of the NPs to the surface regions at high temperature (800 K); thus, the deformation of the NP increases as the temperature increases.

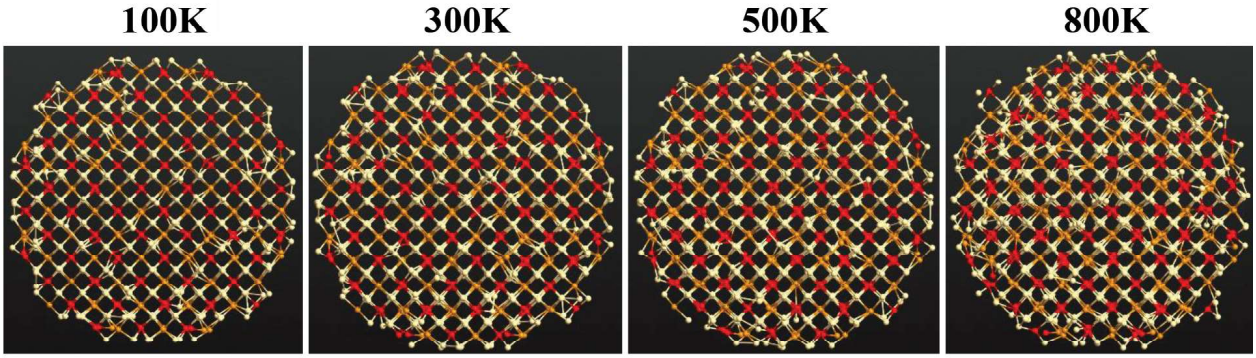

Figure 9. The structures (Cd is gray, Te is orange, and Se is red) of the $CdTe_{0.50}Se_{0.50}$ spherical NP with 2.0 nm at various temperatures.

The potential energy as a function of temperature for various CdTeSe NPs is displayed in Figure 10. In Figure 10, the variation of the average energy represents a linear relationship with the temperature in the range 100–800 K; however, as the NP size increases, a sharp increase is noted. Furthermore, the potential energy decreases depending on the size increase in the NPs at all temperatures due to the stoichiometry of the surface atoms in the NPs.

The C_v is expressed with the relationship between the internal energy and temperature:

$$C_v = \left(\frac{\partial E}{\partial T}\right)_v .$$

In this study, the internal energy is associated with the interaction potential energy. The calculations of C_v of CdTeSe NPs with different sizes and compositions, for the first time, have been investigated using MD simulations. Figure 11 shows the behavior of C_v with respect to NP size and composition. For $CdTe_{1-x}Se_x$ (x = 0.25, 0.50, and 0.75), C_v with respect to size does not indicate a sharp increase up to NPs with 1.4 nm. After that, it shows a sharp increase in accordance with the increase in the NP size. This behavior can be explained by the core and surface atoms because the surface atoms have lower proportions with the increase in the NP size. The monotonically increasing trend of C_v with the increase in the number of atoms is related to the composition of Te atoms when the sizes of NPs are considered [40,41]. In addition, C_v has a minimum value for $CdTe_{0.75}Se_{0.25}$ NP with 1.0 nm and a maximum value for $CdTe_{0.75}Se_{0.25}$ NP with 2.0 nm. The obtained results indicate that the size and composition of the Te and Se atoms have a strong impact on the C_v. This dependence of C_v for ternary $CdTe_{1-x}Se_x$ alloys was also observed in the experimental study by Predeep et al. [42]. In this regard, the photovoltaic performance mainly resulted from the influence of nanocrystal composition on the charge separation [43], which depends on the match of the band level positions because the difficulty of charge separation should be the main reason for the poor photovoltaic performance of the solar

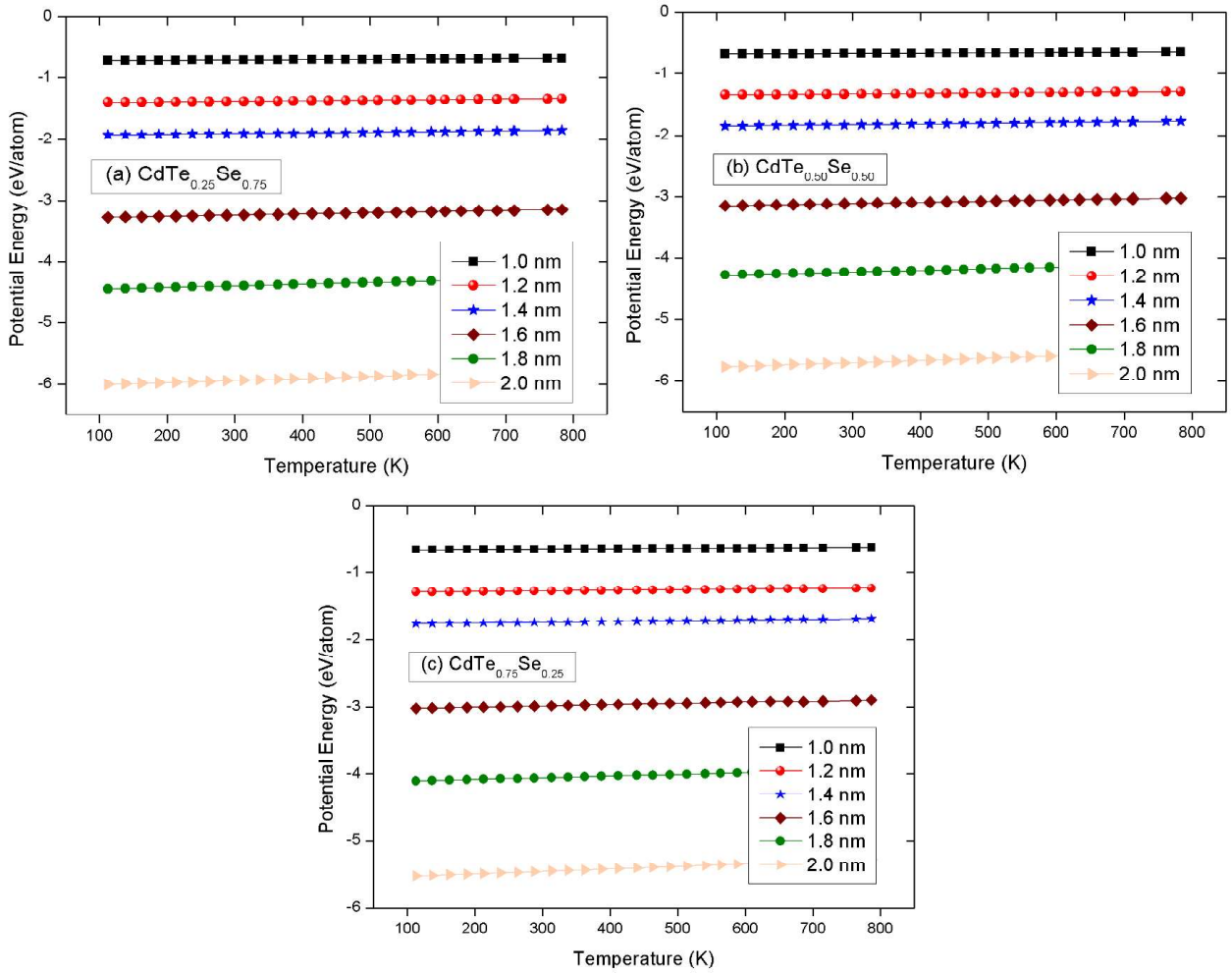

Figure 10. Behavior of potential energy as a function of temperature according to the size and stoichiometry of NPs: $CdTe_{0.25}Se_{0.75}$ (a), $CdTe_{0.50}Se_{0.50}$ (b), and $CdTe_{0.75}Se_{0.25}$ (c).

cells. For example, the photovoltaic properties of the solar cells based on the CdTe and CdSe nanocrystals show big differences. A good arrangement in the composition of Se atoms may contribute to the efficiency of solar cell applications.

4. Conclusion

We investigated the size- and composition-dependent structure of ternary zinc-blende $CdTe_{1-x}Se_x$ NPs using MD simulations with BOP for the first time. The compositional variations of Cd, Te, and Se atoms along with order parameter, radial distribution function, potential energy, and heat capacity were studied. Se atoms had a significant effect on the stability of $CdTe_{1-x}Se$ NPs. Some incorporation of Te and Se inside the core was observed. The value of C_v based on size increased with the decrease in the composition of Te atoms. Se atoms contributed significantly to stability. In addition, Cd-Se had a narrower and higher distribution than the other pair interactions due to the weaker bond and the low atomic weight of the Se atom. The coordination number

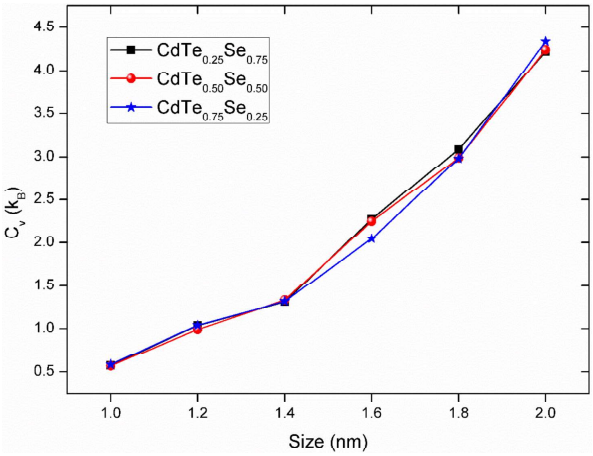

Figure 11. Size and composition dependence of C_v for $CdTe_{1-x}Se_x$ (x = 0.25, 0.50, and 0.75) NPs in the temperature range of 100–800 K.

with respect to probability distribution increased in line with the increase in temperature. The simulation results were also compatible with the available experimental results.

Acknowledgments

This work was supported by the Ahi Evran University Scientific Research Projects Coordination Unit (Project Number: TBY.C1.17.001). The numerical calculations reported in this paper were partially performed at the TÜBİTAK ULAKBİM High Performance and Grid Computing Center (TRUBA resources).

References

[1] Wang, C. L.; Zhang, H.; Zhang, J. H.; Li, M. J .; Sun, H. Z.; Yan, B. *J. Phys. Chem. C* **2007**, *111*, 2465-2469.

[2] Yang, P.; Tretiak, S.; Masunov, A. E.; Ivanov, S. *J. Chem. Phys.* **2008**, *129*, 74709.

[3] Kushwaha, A. K. *Comp. Mater. Sci.* **2012,** *65*, 315-319.

[4] Gupta, A.; Parikh, V.; Compaan A. D. *Sol. Energ. Mat. Sol. C* **2008**, *90*, 2263-2271.

[5] Melnikov, A. A. *J. Cryst. Growth* **1999**, *197*, 663-665.

[6] Li, S.; Jiang, Y.; Wu, D.; Wang, B.; Li, J.; Zhang, Y.; Wang, W.; Lan, X.; Zhong, H.; Chen, L. *Mater. Lett.* **2011**, *65*, 1753-1755.

[7] Mandal, K. C.; Kang, S. H.; Choi, M.; Mertiri, A.; Noblitt, C.; Smirnov, A. *Mater. Res. Soc. Symp. P.* **2008**, *1038*, 39-49.

[8] Eisen, Y.; Shor, A.; Mardor, I. *Nucl. Instrum. Meth. A* **1999**, *428*, 158-170.

[9] Surendra, K. S.; Jagannath, V. T.; Deepak, P. D.; Vijay, J. F. *Appl. Surf. Sci.* **2013**, *282*, 561-565.

[10] Zhong, X.; Feng, Y.; Zhan, Y.; Gu, Z.; Zou, L. *Nanotechnology* **2007**, *18*, 385606.

[11] Hannachi, L.; Bouarissa, N. *Superlattice. Microst.* **2008**, *44*, 794-801.

[12] Yu, T. C.; Brebrick R. F. *J. Phase Equilib.* **1992**, *13*, 476-496.

[13] Johnson, C. J. *SPIE* **1989**, *1106*, 56-68.

[14] Kim, K. H.; Hong, J. K.; Kim, S. U. *J. Cryst. Growth* **2008**, *310*, 91-95.

[15] Poplawsky, J. D.; Guo, W.; Paudel, N.; Ng, A.; More, K.; Leonard, D.; Yan, Y. *Nat. Commun.* **2016**, *7*, 12537.

[16] Paudela, N. R.; Yanb, Y. *Appl. Phys. Lett.* **2014**, *105*, 183510.

[17] Lennard-Jones, J. E. *Proc. R. Soc. Lon. Ser-A* **1930**, *129*, 598-615.

[18] Axilrod, B. M.; Teller, E. *J. Chem. Phys.* **1943,** *11*, 299-300.

[19] Kurban, M.; Erkoç, Ş. *Research & Reviews: Journal of Pure and Applied Physics* **2013**, *1*, 35-42.

[20] Kurban, M.; Erkoç, Ş. *J. Comput. Theor. Nanos.* **2015**, *12*, 2605-2615.

[21] Kurban, M.; Erkoç, Ş. *Quantum Matter* **2016**, *5*, 602-605.

[22] Kurban, M.; Malcıoğlu, O. B.; Erkoç, Ş. *Chem. Phys.* **2016**, *464*, 40-45.

[23] Kurban, M.; Erkoç, Ş. *Comp. Mater. Sci.* **2016**, *122*, 295-300.

[24] Kurban, M.; Erkoç, Ş. *Physica E* **2017**, *88*, 243-251.

[25] LAMMPS, lammps.sandia.gov/download.

[26] Plimpton, S. *Comput. Phys.* **1995**, *117*, 1-19.

[27] Zhou, X. W.; Foster, M. E.; van-Swol, F. B.; Martin, J. E.; Wong, B. M. *J. Phys. Chem. C* **2014**, *118*, 20661-20679.

[28] Ward, D. K.; Zhou, X. W.; Wong, B. M.; Doty, F. P.; Zimmerman, J. A. *J. Chem. Phys.* **2011**, *134*, 244703.

[29] Ward, D. K.; Zhou, X. W.; Wong, B. M.; Doty, F. P.; Zimmerman, J. A. *Phys. Rev. B* **2012**, *85*, 115206.

[30] Pettifor, D. G.; Finnis, M. W.; Nguyen-Manh, D.; Murdick, D. A.; Zhou, X. W.; Wadley, H. N. G. *Mater. Sci. Eng. A* **2004**, *365*, 2-13.

[31] Pettifor, D. G.; Oleinik, I. I. *Phys. Rev. Lett.* **2000**, *84*, 4124-4127.

[32] Pettifor, D. G.; Oleinik, I. I. *Phys. Rev. B* **2002**, *65*, 172103.

[33] Drautz, R.; Murdick, D. A.; Nguyen-Manh, D.; Zhou, X. W.; Wadley, H. N. G.; Pettifor, D. G. *Phys. Rev. B* **2005**, *72*, 144105.

[34] Nosé, S. *J. Chem. Phys.* **1984**, *81*, 511-519.

[35] Hoover, W. G. *Phys. Rev.* **1985**, *A31*, 1695-1697.

[36] Yang, P.; Cao, Y.; Li, X.; Zhang, R.; Liu, N.; Zhang, Y. *Luminescence* **2016**, *29*, 407-409.

[37] Lu, C.; Cheng, Y.; Pan, Q.; Tao, X.; Yang, B.; Ye, G. *Sci. Rep-UK* **2016**, *6*, 19870.

[38] Wu, G. H.; Liu, Q. M.; Wu, X. *Chem. Phys. Lett.* **2015**, *620*, 92-97.

[39] Hung, L. X.; Thang, P. N.; Nong, H. V.; Yen, N. H.; Chinh, V. Đ.; Vu, L. V.; Hien, N. T. T.; de Marcillac, W. D.; Hong, P. N.; Loan, N. T. et al. *J. Electron. Mater.* **2016**, *45*, 4425-4431.

[40] Cohen, M. H.; Grest, G. S. *Phys. Rev. B* **1979**, *20*, 1077-1098.

[41] Cornet, J.; Rossier, D. *J. Non-cryst. Solids* **1973**, *12*, 61-84.

[42] Predeep, P.; Saxena, N. S.; Saksena, M. P.; Kumar, A. *Phys. Status Solidi A* **1996**, *155*, 333-339.

[43] Zhou, Y.; Li Y.; Zhong, H.; Hou, J.; Ding, Y.; Yang, C.; Li, Y. *Nanotechnology* **2006,** *17*, 4041-4047.